

High-resolution x-ray microstructural study of single crystals of $\text{YBa}_2\text{Cu}_3\text{O}_{7-\delta}$

Hoydoo You and J. D. Axe

Department of Physics, Brookhaven National Laboratory, Upton, New York 11973

X. B. Kan and S. C. Moss

Physics Department, University of Houston, Houston, Texas 77004

J. Z. Liu and D. J. Lam

Materials Science Division, Argonne National Laboratory, Argonne, Illinois 60439

(Received 30 September 1987)

Single crystals of $\text{YBa}_2\text{Cu}_3\text{O}_{7-\delta}$ were studied by transmission Laue photography and monochromatic diffraction techniques, using the Cornell High Energy Synchrotron Source and a conventional rotating anode x-ray source. Two types of twinning were observed: the well-known (110)-type twinning in one sample and a 90° twinning about the c axis in another crystal whose superconducting properties were excellent, thereby precluding the necessity of (110) twins for high T_c . Diffraction experiments on the sample with the (110) twins reveal subgrains, each of which has a value of the orthorhombic parameter $(a-b)/a$ differing by as little as 0.003 from the others. Such a microstructure distribution suggests a multiphase character and is discussed in relation to recent evidence of granular superconductivity.

Since the discovery¹ of superconductivity above 90 K in the Y-Ba-Cu-O system, several electron microscopy,²⁻⁵ x-ray diffraction,⁶⁻⁹ and neutron-diffraction,¹⁰⁻¹⁴ studies have been made and the structure of the phase responsible for superconductivity is now agreed to be an orthorhombic, tripled perovskite structure, $\text{YBa}_2\text{Cu}_3\text{O}_{7-\delta}$ with $\delta \approx 0.1$ and no oxygen atoms in the Y plane. Within the Cu-O basal plane, it is also known from neutron-powder¹¹⁻¹⁴ and single-crystal¹⁰ diffraction studies that oxygen atoms preferentially order (form chains) along one of the two bridge sites, resulting in 1%–2% larger lattice constant along the chain. In all single-crystal studies, it has been reported either that the crystals are heavily twinned^{5,7,9,10} or that the structure is unstable and easily breaks into twin domains under mechanical stress.¹⁵ When single crystals were found without twinning, a somewhat different ratio of a and b lattice constants (~ 1.10) from that found in powder diffraction studies (~ 1.16) was reported.¹⁵ It is also clear that a and b depend on the basal plane oxygen content.^{16,17} The subject of twinning defects in this material has been investigated in several electron-microscopy studies,²⁻⁴ where it was reported that twinning is mostly of the conventional (110) type. However, occasionally other types of twinning [involving 90° or 180° domains as observed in ferroelectric BaTiO_3 (Ref. 18)] are also discussed.²⁻⁴ In the present paper, we report on two distinct types of twinning in superconducting crystals of $\text{YBa}_2\text{Cu}_3\text{O}_{7-\delta}$. We also show that our (110) twinned crystal is actually composed of several domains or subgrains, with slightly differing orthorhombic parameters, $\eta = (a-b)/a$, which may be formally ascribed to an inhomogeneity of oxygen ordering.

The sample crystals were grown from a mixture of pure Y_2O_3 , BaCO_3 , and CuO in stoichiometric ratio Y:Ba:Cu = 1:2:3 by the solid-state sintering method used for the previous studies.^{10,19} Two sample crystals of $\sim 0.3 \times 0.2$

$\times 0.1 \text{ mm}^3$ (sample I) and $\sim 0.2 \times 0.2 \times 0.05 \text{ mm}^3$ (sample II) were examined with transmission Laue photography and counter diffraction methods using the Cornell High Energy Synchrotron Source (CHESS) and a laboratory rotating anode source. For Laue photography, the samples were exposed to a white x-ray beam, for a few milliseconds at CHESS and several hours at the 10-kW rotating anode, to produce patterns on flat films (either Kodak DEF5 or Polaroid 57). After orientation along a high-symmetry direction, the observed pattern was compared to ones graphically produced, which included various hypothetical types of twinning, using the expression

$$X, Y = \frac{2Q_x Q_y Q_z}{Q_x^2 + Q_y^2 - Q_z^2},$$

where X and Y are spot positions on the film (in units of the sample film distance) with the incoming x-ray beam along the Z direction and Q_x , Q_y , and Q_z are momentum components of a given reflection, and which can be readily derived from the Laue diffraction geometry.

Because the crystals were so small they served as a limiting slit to provide high angular resolution in our Laue photos. It is straightforward to find a twinning model corresponding to the observed pattern. The observed and calculated patterns for the two samples are shown in Fig. 1 (sample I) and in Fig. 2 (sample II). The size of circles in the calculated patterns [Figs. 1(c) and 2(b)] approximately represents the relative intensities of reflections within the reciprocal volume of $\pm 4 \pm 4 \pm 12$ in hkl units calculated from the known structure of this material.¹⁰ Overall agreement of the spot intensities is satisfactory although calculated intensities do not accurately represent observed spot sizes on the photos because of (i) the non-linear response of film to exposure, (ii) not including all possible reflections, and (iii) dependence of source x-ray intensities upon wavelength.

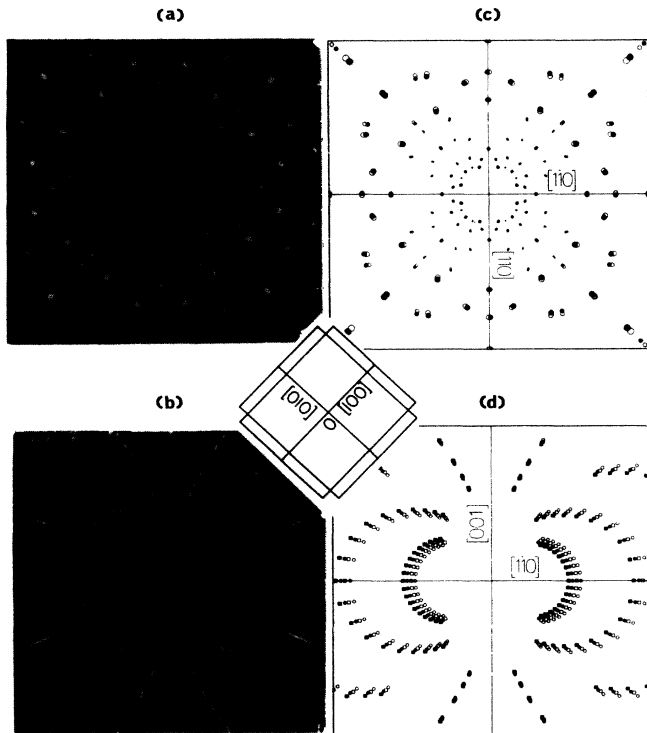


FIG. 1. Transmission white beam Laue photos and calculated patterns for sample I. (a) and (c) are for the incident x-ray beam along $[001]$ direction, and (b) and (d) are for the incident x-ray beam along $[110]$ direction. The inset shows the way of overlapping the reciprocal lattice to produce the calculated pattern due to twins that are rotated by 90° about the c axis. (In the transmission, Laue method spots from the planes of a zone lie on ellipses or hyperbolas.) See the text for discussion.

For sample I, whose crystal structure was determined in Ref. 10, photographs taken with the incident x-ray beam along a $[001]$ direction [Fig. 1(a)] and along a $[110]$ direction [Fig. 1(b)] are shown. In these photos, most of spots are split and reflections in Fig. 1(b) are (nearly) radially elongated. Figure 1(c) is produced to give the best fit to Fig. 1(a) by overlapping two domains which are rotated exactly 90° from each other about the common c axis (see the inset of Fig. 1). We refer to this as 90° twinning in which the reflections along $\langle 100 \rangle$ or $\langle 010 \rangle$ directions split only radially while ones along $\langle 110 \rangle$ or $\langle 1\bar{1}0 \rangle$ directions split only azimuthally. In the calculated pattern [Fig. 1(c)], reflections from one of the twin domains are represented by open circles and ones from the other are given as closed circles. A close examination of the photo reveals that the set of reflection intensities from one domain is weaker than from the other with the relative intensities of split peaks, in reasonable agreement with those of the calculated pattern [Fig. 1(c), open circles for the weak spots and closed circles for the strong ones]. Figure 1(d) is calculated for x rays incident along the $[110]$ direction with the same 90° twin domains. In addition to the twin domains, however, it was assumed that each twin domain has a mosaic distribution with a total misorientation of 0.5° . This is shown schematically in Fig. 1(d) by

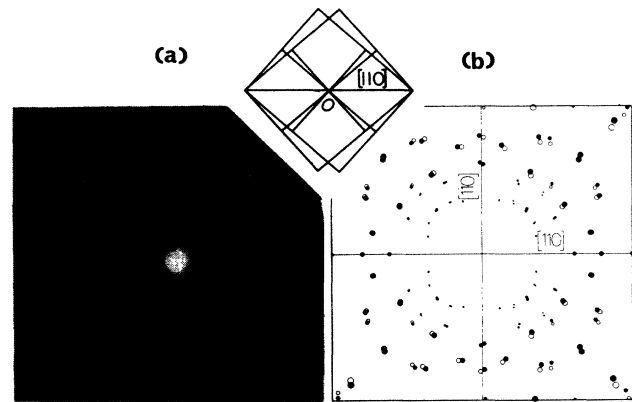


FIG. 2. Laue photo and calculated pattern for sample II. The inset shows a schematic reciprocal lattice associated with twinning across the $[110]$ direction in which the $[110]$ directions are parallel in the two twins. See the text for discussion.

two mosaic blocks (circles and squares) separated by 0.5° . The similarity of the calculated pattern [Fig. 1(d)] to the observed one [Fig. 1(b)] suggests that the (nearly) radial elongation of the reflections is probably due to a mosaic distribution about the c axis and/or strain at the twin boundaries. [The 0.5° mosaic spread is, of course, the same in Fig. 1(a) as in Fig. 1(c). It is, however, exaggerated in the latter because of the way it is projected onto the film.] Because of the homogeneous nucleation associated with the tetragonal to orthorhombic transition which occurs at $\sim 700^\circ\text{C}$ (Refs. 17 and 20) the orthorhombic domains in different regions (for example, along the c axis) can randomly form by alternating a and b along the $\langle 100 \rangle$ or $\langle 010 \rangle$ tetragonal axis. It is, however, by no means evident how such domains are interconnected within the single crystallite. The absence of (110) twins in sample I, which showed excellent superconducting properties,¹⁹ also precludes the necessity of (110) twinning for high T_c .

In sample II, Laue photography with rotating anode x rays reveals the more conventional type of twinning, where the twin boundaries run perpendicular to the $[110]$ direction. This type of twinning is common because (110) planes aligned across the twin boundaries minimize elastic strain energy and it therefore involves only short-range oxygen-oxygen (chemical) interaction energy.²¹ The resulting Laue pattern should show unsplit reflections along the $[110]$ direction and maximum azimuthal splitting along the $[1\bar{1}0]$ direction as shown in Fig. 2. In addition to this expected splitting, we also observed slight misalignments of the split peaks. The misalignment in this case was well produced in Fig. 2(b) with a 0.2° rotation of domains about the $[110]$ axis and this is confirmed in additional diffraction experiments described below. The Laue photos taken for the $[110]$ direction parallel to the incident x rays (not reproduced here) also show radial elongation similar to the case of sample I and caused by mosaic distribution of $\sim 0.5^\circ$ about the c axis.

Sample II was studied as well as CHESS beam line A2 in a four-circle diffractometer using focused 17-keV x rays

with a vertical scattering geometry. Initial experiments were concerned with possible diffuse scattering in the Bragg wings, which would occur normal to the domain boundaries in the event of appreciable strain or lattice spacing variation. Since scans with modest momentum resolution are more useful in detection of diffuse scattering than is high resolution, no analyzer crystal was used. Scans were always made in one of three simple zones ($\{110\}$, $\{001\}$, or $\{100\}$) to ensure that the direction of the resolution ellipsoid was known. Scans were made about several Bragg peaks, but no prominent diffuse scattering was observed. A domain size of ~ 500 Å could be deduced from the widths of Bragg peaks along all directions.

When scans were made in the $\{001\}$ zone, remarkable asymmetry in the azimuthal profile was observed. As an example, the ω scans at (440) and $(4\bar{4}0)$ (made by rotating the crystal through its reflection at fixed detector angle) are shown in Fig. 3. Because of the very high transverse q resolution of well-collimated synchrotron x rays, the detailed azimuthal distribution was clearly revealed in these scans. The $(4\bar{4}0)$ reflection is composed of at least 10 peaks distributed azimuthally along the arc (see the inset) for the range of 2° – 3° while the (440) reflection is essentially simple. (Although it is not evident in Fig. 2, the original Laue photographs also show a wealth of fine structure that is consistent with that observed by a four-circle diffractometer.) Out-of-plane scans made at (440) showed no structure, indicating that the structured azimuthal profile is only for $(4\bar{4}0)$ reflection and mainly in the $\{001\}$ zone.

One possible explanation for this structured azimuthal profile of a (440) reflection is an interference effect due to a periodic domain distribution along the $[110]$ direction as theoretically suggested in this class of material.²² This requires that the spacing between these peaks be regular in reciprocal lattice, or (hkl) , units (not in angle). Scans were therefore made for (550) and (660) reflections and the observed *angular* structures of these scans were very similar to that of a $(4\bar{4}0)$ reflection, thereby excluding a

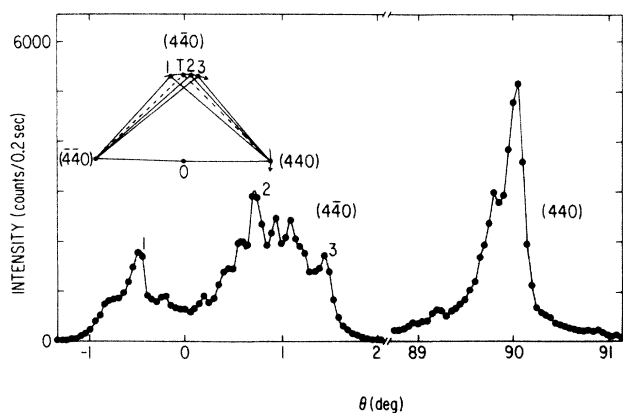


FIG. 3. ω scans made at (440) and $(4\bar{4}0)$ reflections. Markedly different azimuthal profiles are the key to our discussion in the text. The directions of scans are schematically shown as arrows on the arc in the inset. Lines are guides to the eye.

periodic twin lattice along $[110]$. It appears therefore that the individual peaks must come from many (presumably) incoherent subgrains with sizes of ~ 500 Å. Given that the structure is orthorhombic and the angle between a and b axes is 90° , the only possible interpretation of the angular distribution in Fig. 3 is that each block or domain has its own value of orthorhombic parameter $\eta = (a-b)/a$. The numbers 1, 2, and 3 shown in the inset schematically illustrate the positions 1, 2, and 3 of the scan profile in the $hk0$ plane. Since there are only small orthorhombic distortions, η also measures the deviation angle in radians from the tetragonal position as marked by T in the inset. The values of η for domains 1, 2, and 3 are -0.008 , 0.012 , and 0.024 , respectively, while only two values of $\eta = \pm |\eta_0|$ are allowed for the ideal (110) twin domains. The nearest peaks have a difference in η of as little as 0.003 or of 0.01 Å in $(a-b)$. To lowest order, azimuthal splitting of $(h\bar{h}0)$ reflections results from variations of $(a-b)$, and thus presumably from variations in oxygen ordering. Radial $(h\bar{h}0)$ splitting or broadening, on the other hand, reflects fluctuations in $(a+b)$. Our failure to observe radial broadening or splitting, limited by instrumental resolution [$\Delta Q/Q = \sim 5 \times 10^{-4}$ with Ge(111) analyzer crystal], places a limit on fluctuations in $(a+b)$ at $\sim 2 \times 10^{-3}$ Å. Thus variations in oxygen ordering, not oxygen stoichiometry, appear to be principally responsible for the variations between such domains; any associated fluctuations in $(a+b)$ are below the limits of detection in this experiment.

Although our samples, grown slowly, show only one type of twinning in one crystal, both types of twinning can happen simultaneously in a crystal.¹⁷ In a recent paper on ordering and decomposition in $\text{YBa}_2\text{Cu}_3\text{O}_{7-\delta}$ Khachatryan and Morris²³ display a schematic phase diagram, in which, at temperatures below the tetragonal to orthorhombic transition for off-stoichiometric compositions, the orthorhombic phase separates into a mixture of ordered orthorhombic and disordered tetragonal phases in a fully developed thermal equilibrium condition. This type of decomposition will involve twin-related orthorhombic domains embedded in a tetragonal matrix of lower oxygen content. The concentration in each domain will depend on heat treatment and cooling rate. Such a phenomenological treatment of decomposition²³ in $\text{YBa}_2\text{Cu}_3\text{O}_{7-\delta}$ may provide a possible origin for different types of twins, such as (110) and 90° twinning as well as a possible inhomogeneity of oxygen content and ordering across the crystallographic domain boundaries in a slowly cooled sample. The postulated phase decomposition is also reminiscent of our earlier observation on the multiphase constitution of $\text{La}_{1.8}\text{Ba}_{0.2}\text{CuO}_{4-\delta}$ (Ref. 24) which showed distinct phase separation on a fine scale.

The inhomogeneous microstructural properties observed in the present study may be related to a recent observation of granular superconductivity,²⁵ where the authors observe a discrete distribution of superconducting transition temperatures starting from as high as ~ 160 K for individual grains. Isolation of the grains or domains with a particular microstructure might well be a key to understanding the relation of microstructure to superconductivity.

We wish to thank the staff at CHESS for their help and, in particular, Dr. W. Schildkamp for assistance in setting up the transmission Laue camera. The work at the Brookhaven and Argonne National Laboratories was supported by the Department of Energy (DOE) under Contracts No. DE-AC02-76CH00016 and No. W-31-109-ENG-38, respectively, and the work at Houston was supported by the NSF on DMR-8603662.

-
- ¹M. K. Wu, J. R. Ashburn, C. J. Torng, P. H. Hor, R. L. Meng, L. Gao, Z. J. Huang, Y. Q. Wang, and C. W. Chu, *Phys. Rev. Lett.* **58**, 908 (1987).
- ²C. H. Chen, D. J. Werder, S. H. Liou, J. R. Kwo, and M. Hong, *Phys. Rev. B* **35**, 8767 (1987).
- ³H. W. Zandbergen, G. Van Tendeloo, T. Okabe, and S. Amelinckx, *Solid State Commun.* (to be published).
- ⁴A. Ourmazd, J. A. Rentschler, J. C. H. Spence, M. O'Keeffe, R. J. Graham, D. W. Johnson, and W. W. Rhodes, *Nature* **327**, 308 (1987).
- ⁵R. Beyers, G. Lim, E. M. Engler, R. J. Savoy, T. M. Shaw, T. R. Dinger, W. J. Gallagher, and R. L. Sandstrom, *Appl. Phys. Lett.* **50**, 1918 (1987).
- ⁶R. J. Cava, B. Batlogg, R. B. van Dover, D. W. Murphy, S. Sunshine, T. Siegrist, J. P. Remeika, E. A. Rietman, S. Zahurak, and G. P. Espinosa, *Phys. Rev. Lett.* **58**, 1676 (1987).
- ⁷R. M. Hazen, L. W. Finger, R. J. Angel, C. T. Prewitt, N. L. Ross, H. K. Mao, C. G. Hadidiacos, P. H. Hor, R. L. Meng, and C. W. Chu, *Phys. Rev. B* **35**, 7238 (1987).
- ⁸T. Siegrist, S. Sunshine, D. W. Murphy, R. J. Cava, and S. M. Zahurak, *Phys. Rev. B* **35**, 7137 (1987).
- ⁹H. Steinfink, J. S. Swinnea, Z. T. Sui, H. M. Hsu, and J. B. Goodenough, *J. Am. Chem. Soc.* (to be published).
- ¹⁰H. You, R. K. McMullan, J. D. Axe, D. E. Cox, J. Z. Liu, G. W. Crabtree, and D. J. Lam, *Solid State Commun.* **64**, 739 (1987).
- ¹¹D. E. Cox, A. R. Moodenbaugh, J. J. Hurst, and R. H. Jones, *J. Phys. Chem. Solids* (to be published).
- ¹²J. J. Capponi, C. Chaillout, A. W. Hewat, P. Lejay, M. Marezio, N. Nguyen, B. Raveau, J. Soubeyroux, J. L. Tholence, and R. Tournier, *Europhys. Lett.* **3**, 1301 (1987).
- ¹³M. A. Beno, L. Soderholm, D. W. Capone, D. G. Hinks, J. D. Jorgensen, I. K. Schuller, C. U. Segre, K. Zhang, and J. D. Grace, *Appl. Phys. Lett.* **51**, 57 (1987).
- ¹⁴F. Beech, S. Miraglia, A. Santoro, and R. S. Roth, *Phys. Rev. B* **35**, 8778 (1987).
- ¹⁵T. R. Dinger, T. K. Worthington, W. J. Gallagher, and R. L. Sandstrom, *Phys. Rev. Lett.* **58**, 2687 (1987).
- ¹⁶J. D. Jorgensen, M. A. Beno, D. G. Hinks, L. Soderholm, K. J. Volin, R. L. Hitterman, J. D. Grace, Ivan K. Schuller, C. N. Segre, K. Zhang, and M. S. Kleefisch, *Phys. Rev. B* **36**, 3608 (1987).
- ¹⁷P. Strobel, J. J. Capponi, C. Chaillout, M. Marezio, and J. L. Tholence, *Nature* **327**, 306 (1987).
- ¹⁸T. Mails and H. Gleiter, *J. Appl. Phys.* **47**, 5195 (1976).
- ¹⁹J. Z. Liu, G. W. Crabtree, A. Umegawa, and Li Zongquau, *Phys. Lett. A* **121**, 305 (1987).
- ²⁰R. Beyers, G. Lim, E. M. Engler, V. Y. Lee, M. L. Ramirez, R. J. Savoy, R. D. Jacowitz, T. M. Shaw, S. La Placa, R. Boehme, C. C. Tsuei, Sung I. Park, M. W. Shafer, W. J. Gallagher, and G. V. Chandrasekhar, *Appl. Phys. Lett.* **51**, 614 (1987).
- ²¹D. de Fontaine, L. T. Wille, and S. C. Moss, *Phys. Rev. B* **36**, 5709 (1987).
- ²²G. R. Barsch, B. Horovitz, and J. A. Krumhansl, *Phys. Rev. Lett.* **59**, 1251 (1987), and references therein.
- ²³S. C. Moss, K. Foster, J. D. Axe, H. You, D. Hohlwein, D. E. Cox, R. L. Meng, P. H. Hor, and C. W. Chu, *Phys. Rev. B* **35**, 7195 (1987).
- ²⁴A. G. Khachatryan and J. W. Morris, Jr., *Phys. Rev. Lett.* **59**, 2776 (1987).
- ²⁵X. Cai, R. Joynt, and D. C. Larbalestier, *Phys. Rev. Lett.* **58**, 2798 (1987).

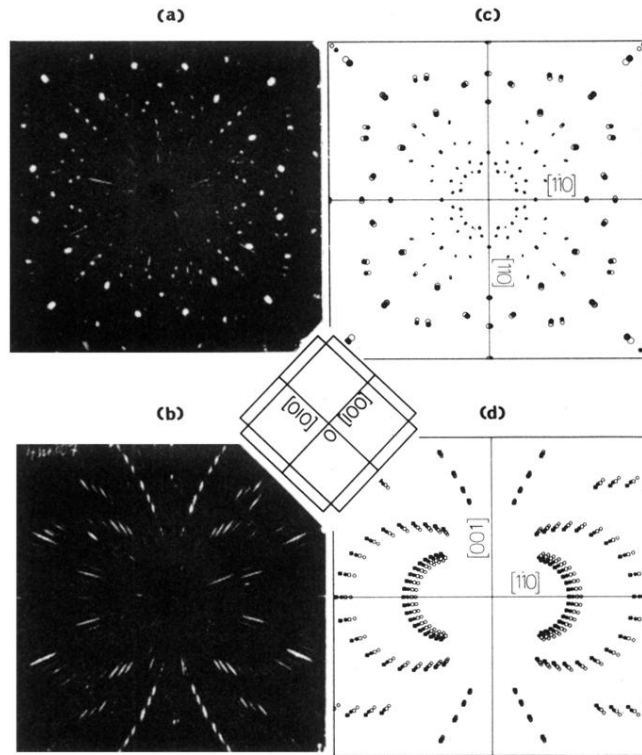


FIG. 1. Transmission white beam Laue photos and calculated patterns for sample I. (a) and (c) are for the incident x-ray beam along $[001]$ direction, and (b) and (d) are for the incident x-ray beam along $[110]$ direction. The inset shows the way of overlapping the reciprocal lattice to produce the calculated pattern due to twins that are rotated by 90° about the c axis. (In the transmission, Laue method spots from the planes of a zone lie on ellipses or hyperbolas.) See the text for discussion.

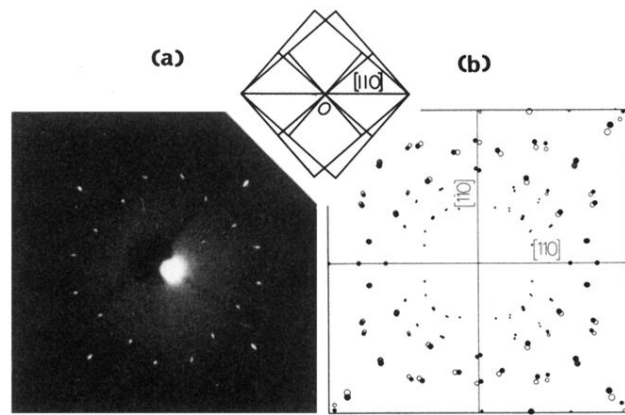


FIG. 2. Laue photo and calculated pattern for sample II. The inset shows a schematic reciprocal lattice associated with twinning across the $[110]$ direction in which the $[110]$ directions are parallel in the two twins. See the text for discussion.